

Efficient Method for Quantum Number Projection and Its Application to Tetrahedral Nuclear States

Shingo TAGAMI¹, Yoshifumi R. SHIMIZU¹, and Jerzy DUDEK²

¹*Department of Physics, Faculty of Sciences, Kyushu University, Fukuoka 812-8581, Japan*

²*Institut de Recherches Subatomiques, IN₂P₃-CNRS/Université Louis Pasteur, F-67037 Strasbourg, France*

We have developed an efficient method for quantum number projection from most general HFB type mean-field states, where all the symmetries like axial symmetry, number conservation, parity and time-reversal invariance are broken. Applying the method, we have microscopically calculated, for the first time, the energy spectra based on the exotic tetrahedral deformation in ^{108,110}Zr. The nice low-lying rotational spectra, which have all characteristic features of the molecular tetrahedral rotor, are obtained for large tetrahedral deformation, $\alpha_{32} \gtrsim 0.25$, while the spectra are of transitional nature between vibrational and rotational with rather high excitation energies for $\alpha_{32} \approx 0.1 - 0.2$.

§1. Introduction

The progress of radioactive beam facilities in these years provides us a great possibility to explore nuclear regions with various combinations of neutron and proton numbers, where many interesting new phenomena have been predicted. In the present work, we would like to focus, among others, on the exotic shape with high rank point group symmetry,¹⁾ i.e., the tetrahedral nuclear states. This “pyramid-like” shape leads to the extra stability in shell energy due to the higher symmetry, e.g., the appearance of fourfold degenerate orbits. It has been suggested that such states appear as low-lying states, or even as a ground state, in some nuclei around the “tetrahedral-closed shell” nuclei;²⁾ see also Refs. 3), 4), 5), 6). In these earlier studies, the mean-field approaches are employed to search for minimum configurations with the tetrahedral shape. However, the quantum excitation spectra and the properties of electromagnetic transition rates between them are necessary to definitely identify the tetrahedral states. The quantum number projection, especially the angular momentum projection, from mean-field states is useful for such a purpose.

Note that the tetrahedral shape is neither axially symmetric nor reflection symmetric; the number conservation is lost if the pairing correlation is included, and the time-reversal invariance is broken if the cranking procedure is used to investigate the collective rotational bands. Therefore, the most general HFB type mean-field states without symmetry restrictions are necessary to describe the tetrahedral nuclei. Recently we have developed an efficient method for quantum number projection from such most general HFB type states.⁷⁾ Employing this method, in this work, we present the quantum spectra of the nuclear tetrahedral rotor, which are obtained microscopically for the first time, and discuss briefly its characteristic properties. More detailed investigations will be reported elsewhere.

§2. Efficient Method for Projection and GCM

Since the detailed information is published in Ref. 7), here we briefly discuss the essential points of our method. The projector is of the form $\hat{P}_\alpha = \int g_\alpha(\mathbf{x}) \hat{D}(\mathbf{x}) d\mathbf{x}$, where $\hat{D}(\mathbf{x})$ is a unitary transformation of symmetry operations, e.g., the rotation, and the main task is to calculate a quantity $\langle \Phi | \hat{O} \hat{D}(\mathbf{x}) | \Phi' \rangle$ for an arbitrary operator \hat{O} and HFB type states $|\Phi\rangle$ and $|\Phi'\rangle$ at the mesh points of integration over the parameter space (\mathbf{x}) . The general HFB state is defined by the quasiparticle operators,

$$\hat{\beta}_k |\Phi\rangle = 0 \quad (k = 1, 2, \dots, M), \quad \hat{\beta}_k^\dagger = \sum_l \left[U_{lk} \hat{c}_l^\dagger + V_{lk} \hat{c}_l \right], \quad (2.1)$$

where $(\hat{c}_l^\dagger, \hat{c}_l)$ are the creation and annihilation operators of the states within the original basis, for which the unitary transformation \hat{D} is represented by a matrix $D = (D_{\nu\mu})$,

$$\hat{D} \hat{c}_l^\dagger \hat{D}^\dagger = \sum_{\nu} D_{\nu l} \hat{c}_\nu^\dagger. \quad (2.2)$$

Then, the quantity $\langle \Phi | \hat{O} \hat{D}(\mathbf{x}) | \Phi' \rangle$ can be expressed in terms of the matrix elements of \hat{O} , the transformation matrix D , (U, V) amplitudes in Eq. (2.1) and the similar amplitudes (U', V') for $|\Phi'\rangle$. All the matrices have sizes $M \times M$ and each matrix manipulation requires $O(M^3)$ operations. This is the difficulty for the projection from the HFB state with a large model space; for example, if we take $N_{\text{osc}}^{\text{max}} = 20$ spherical harmonic oscillator shells, the dimension becomes $M = 3,542$. If the pairing correlation is neglected and the calculation is restricted to the HF state, it is shown that the matrix operations reduces to $O(MN^2)$ for one-body operators, where N is the number of particles and is at most 200 or so.

The method we have taken to circumvent this difficulty can be summarized by the following two points:

- Basis truncation in terms of the canonical basis; with

$$\hat{b}_k^\dagger = \sum_l W_{lk} \hat{c}_l^\dagger, \quad \langle \Phi | \hat{b}_k^\dagger \hat{b}_k | \Phi \rangle = \delta_{kk'} v_k^2 \quad (v_k^2 \text{ in descending order}), \quad (2.3)$$

the P space is defined as $\{k = 1, 2, \dots, L_p(\epsilon); v_k^2 \geq \epsilon\}$ with a small number ϵ .

- Full use of the Thouless form with respect to a Slater determinant;

$$|\Phi\rangle = n \exp \left(\sum_{l>l'} Z_{ll'} a_l^\dagger a_{l'}^\dagger \right) |\phi\rangle, \quad |\phi\rangle \equiv \prod_{k=1}^N b_k^\dagger |0\rangle, \quad a_k^\dagger = \begin{cases} b_k & k \leq N \\ b_k^\dagger & k > N \end{cases}. \quad (2.4)$$

In order to avoid the sign problem of norm overlap for general HFB states,⁸⁾ especially those without the time-reversal invariance, one has to calculate the pfaffian with Thouless amplitudes. Then it is easy to show that the matrix operations for one-body operators can be reduced to $O(ML_p^2(\epsilon))$ by the canonical basis truncation above. However, the Thouless amplitude with respect to nucleon vacuum diverges when the pairing correlation is vanishing or the HFB state is orthogonal to the nucleon vacuum, e.g., a quasiparticle excited state. The Thouless form with respect to

a Slater determinant in Eq. (2.4) solves this difficulty because then the amplitude $Z \sim u_k/v_k$ for $k \leq N$ and $Z \sim v_k/u_k$ for $k > N$ in the diagonal representation, and the truncation scheme can be utilized for any HFB type mean-field states. In addition, the calculation can be further reduced because of the simple treatment of the core space (deep hole states) defined as $\{k = 1, 2, \dots, L_o(\epsilon); u_k^2 = 1 - v_k^2 \geq \epsilon\}$.

Examples of the occupation and empty probabilities, v_k^2 and u_k^2 , are shown in Fig. 1, and the resultant two dimensions, $L_p(\epsilon)$ and $L_o(\epsilon)$, as well as the calculated rotational spectra are shown in Fig. 2. It can be seen that the truncation parameter $\epsilon \approx 10^{-3} - 10^{-4}$ is sufficient, and then the necessary P space dimension is $L_p \approx 150$ ($L_o \approx 50$), which is much smaller than the original basis size $M \approx 3,000$. Thus the calculational effort is dramatically reduced.

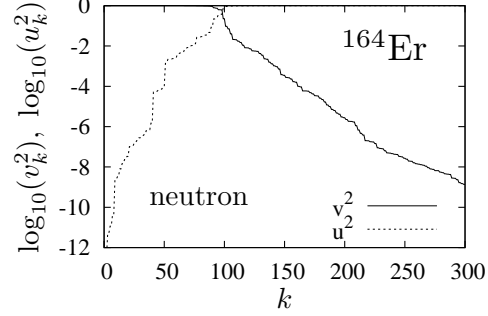


Fig. 1. Probabilities v_k^2 and u_k^2 as functions of the number k of the canonical basis.

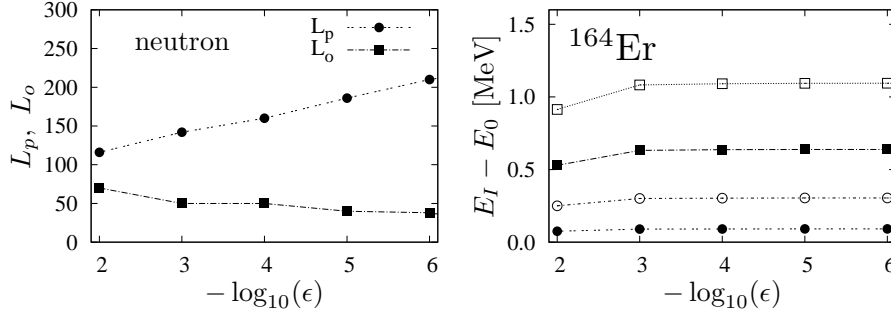


Fig. 2. Dimensions of the P -space L_p and the core space L_o as functions of the model space truncation parameter ϵ (left), and the rotational spectra ($I = 2, \dots, 8$) as functions of the truncation parameter ϵ for ^{164}Er (right).

As for the choice of the Hamiltonian, it may be desirable to employ effective interactions like Skyrme and Gogny forces, but they have problems for the projection and the GCM calculations due to their density-dependence. Thus, for the illustration of our method, we use the following schematic multi-separable interaction:

$$\hat{H} = \hat{h} - \frac{1}{2}\chi \sum_{\lambda} : \hat{F}_{\lambda}^{\dagger} \cdot \hat{F}_{\lambda} : - \sum_{\lambda, \tau=n,p} g_{\lambda}^{\tau} \hat{G}_{\lambda}^{\tau\dagger} \cdot \hat{G}_{\lambda}^{\tau}, \quad (2.5)$$

where the single-particle part \hat{h} is composed of the Woods-Saxon potential. The two-body interaction is constructed from the isoscalar particle-hole channel operators $F_{\lambda\mu} = \sum_{\tau=n,p} F_{\lambda\mu}^{\tau}$ and the pairing channel operators $G_{\lambda\mu}^{\tau}$ defined by

$$F_{\lambda\mu}^{\tau}(\mathbf{r}) = R_0^{\tau} \frac{dV_c^{\tau}(r)}{dr} Y_{\lambda\mu}(\theta, \phi), \quad G_{\lambda\mu}^{\tau}(\mathbf{r}) = \left(\frac{r}{R_0}\right)^{\lambda} \sqrt{\frac{4\pi}{2\lambda+1}} Y_{\lambda\mu}(\theta, \phi), \quad (2.6)$$

with $V_c^{\tau}(r)$ and R_0^{τ} being the central part of the Woods-Saxon potential and its radius parameters, respectively, and $\bar{R}_0 \equiv 1.2A^{1/3}$ fm. The multipolarities $\lambda = 2, 3, 4$

are included in the p-h channel and $\lambda = 0, 2$ in the pairing channel. As for the force strengths, we adopt the selfconsistent value for χ , while the values of g_0^τ are determined according to even-odd mass differences Δ_τ . The ratio $g_2^\tau/g_0^\tau = 13.6$ is chosen to reproduce typical rotational bands in a rare-earth and an actinide nucleus, see Ref. 7) for details. It should be noted that this kind of schematic Hamiltonian cannot be used to obtain the ground state energy and deformation; it is only used to calculate the collective excitation spectra based on a given mean-field state $|\Phi\rangle$.

§3. Spectra of Nuclear Tetrahedral Rotor

The tetrahedra deformation can be conveniently described by the α_{32} deformation without other terms in the usual nuclear surface parametrization,

$$R(\theta, \varphi) = R_0 c_v(\{\alpha\}) \left(1 + \sum_{\lambda\mu} \alpha_{\lambda\mu}^* Y_{\lambda\mu}(\theta, \varphi) \right). \quad (3.1)$$

Thus, it is clear that both the axial symmetry and parity are broken. Now let us investigate what kinds of quantum spectra with definite spin-parity are expected for the tetrahedrally deformed nuclear state. For this purpose, it is interesting to consider the region near one of double tetrahedral-closed shell nuclei, ^{110}Zr ($Z = 40$ and $N = 70$), because experiments for neutron-rich Zr isotopes have been done recently at RIKEN.⁹⁾ In this experiment a new isomer with life time of about 600 nsec has been found in a nucleus ^{108}Zr , and speculated as a possible low-lying tetrahedral state according to a theoretical prediction.¹⁰⁾

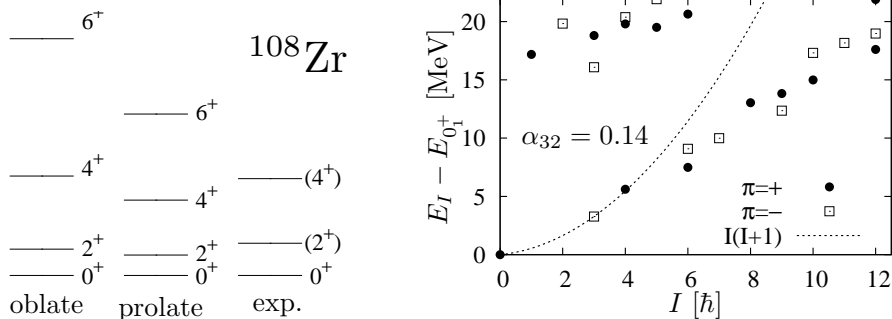


Fig. 3. Calculated spectra of the ground state band in ^{108}Zr (left), and of tetrahedral states assuming $\alpha_{32} = 0.14$ (right). Dotted curves denote the $I(I+1)$ spectra going through 3_1^- . Although higher excited states may not have realistic meaning, they are included to show what kind of spin-parity appears.

We apply our quantum number projection method to $^{108,110}\text{Zr}$ nuclei. In order to obtain a reliable mean-field for the ground states, we have performed the paired Woods-Saxon Strutinsky calculation of Ref. 11) (with the Wyss-2 potential parameter set). Since the pairing model space is cut off in these calculations, we do not include the cut-off factor, which was introduced in Ref. 7) for the pairing operators $G_{\lambda\mu}^\tau$ in Eq. (2.5), in the present projection calculation. The pairing force strength g_0^τ are fixed according to those results with the same ratio $g_2^\tau/g_0^\tau = 13.6$ as previously.

The model space size $N_{\text{osc}}^{\text{max}} = 18$ and the truncation parameter $\epsilon = 10^{-4}$ are used. Because the cranking procedure is important to evaluate the moment of inertia,⁷⁾ we use a small cranking frequency $\hbar\omega_{\text{rot}} = 0.01$ MeV about the x -axis in all calculations.

We compare calculated ground state bands in ^{110}Zr with experimental data⁹⁾ in Fig. 3. Since the total energies of prolate and oblate minima are almost the same, we show spectra on both of them. The oblate spectra better agrees with data, though the prolate ground state energy is slightly lower. In any case, this confirms that our Hamiltonian is a reasonable one. The calculated spectra of tetrahedral states with assumed deformation¹⁰⁾ $\alpha_{32} = 0.14$ are also shown in Fig. 3. Although the spectra are not so rotational-like, their spin-parity appears to be characteristic to the simplest singlet representation of the tetrahedral rotor¹²⁾ corresponding to the closed shell, i.e., 0^+ , 3^- , 4^+ , 6^\pm (doublet), etc., even for a neutron non-closed nucleus ^{110}Zr . This is because the totally symmetric state is realized owing to the pairing correlation. If the pairing is switched off, two neutrons partially fill the last fourfold generate orbit and the resultant Slater determinant is not tetrahedrally symmetric. Then, the spectra are more complex combinations of various irreducible representations.

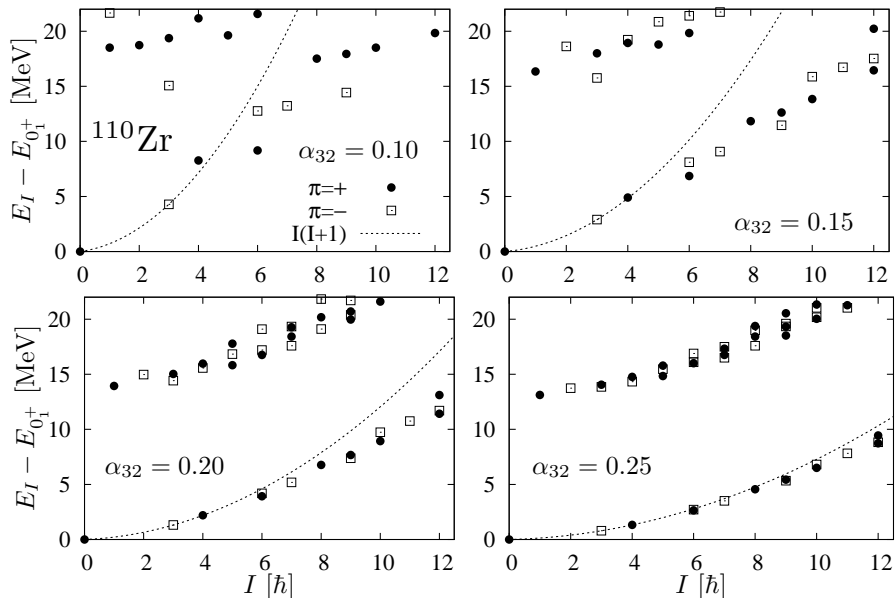


Fig. 4. Calculated spectra of tetrahedral states in ^{110}Zr with various values of α_{32} . These results correspond to projection from a single HFB wave function; the high lying bands serve merely the illustration of the symmetry properties and are not meant to be compared with experiment.

In Fig. 4 the calculated tetrahedral spectra of the double closed nucleus ^{110}Zr , for which the mean-field state is tetrahedrally symmetric and gives the same characteristic spectra even in the unpaired case, are depicted for various values of α_{32} . It is clearly seen that the spectra gradually change to rotational ones at considerable deformation $\alpha_{32} = 0.25$, while they are more like vibrational or transitional in $0.1 \lesssim \alpha_{32} \lesssim 0.20$; the 3_1^- energy quickly decreases as α_{32} increases. This kind of phase transitions is well-known for the quadrupole deformation. We plot the moment of inertia estimated by $6/E(3_1^-)$ in Fig. 5, where the results with switching off the

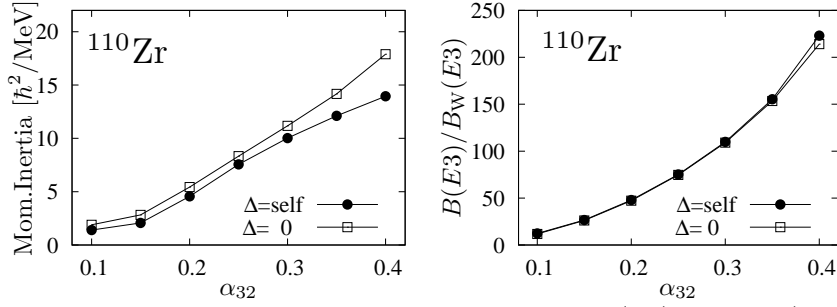


Fig. 5. Calculated moment of inertia deduced from the 3_1^- energy (left) and the $B(E3 : 3_1^- \rightarrow 0_1^+)$ in Weisskopf unit (right) as functions of α_{32} for ^{110}Zr . The rigid-body inertia is $35.1 [\hbar^2/\text{MeV}]$.

pairing correlation are also included. Note that the effect of the pairing correlation is not so strong. This may be partly because this nucleus is double tetrahedral-closed and the pairing gaps of neutron and proton are not so large. Compared to the rigid body value, $\frac{2}{5}AM\bar{R}_0^2 = 35.1 \hbar^2/\text{MeV}$, the moment of inertia is rather small even at $\alpha_{32} \approx 0.4$ without pairing correlation. The calculated $B(E3 : 3_1^- \rightarrow 0_1^+)$ value is also shown in Fig. 5, which well corresponds to the rotor model estimate, $(2 - \delta_{K0})|\langle\Phi|r^3Y_{3K}|\Phi\rangle|^2\langle 3K3 - K|00\rangle^2$, with $K = 2$. Again, they become very large, more than 100 Weisskopf unit, for $\alpha_{32} \gtrsim 0.3$.

In summary, we have calculated the spectra of the nuclear tetrahedral rotor for the first time by employing the quantum number projection method. By increasing the tetrahedral deformation, the spectra gradually change from vibrational to rotational just like in the spherical-to-deformed phase transition in the case of quadrupole deformation. It is quite interesting to measure the characteristic spectra of the tetrahedral rotor, which is a clear indication of the exotic tetrahedral deformation in atomic nuclei.

Acknowledgements

This work is supported by Grant-in-Aid for Scientific Research (C) No. 22540285 from Japan Society for the Promotion of Science.

References

- 1) J. Dudek, A. Gózdź, K. Mazurek, and H. Molique, *J. Phys. G* **37** (2010), 064032.
- 2) J. Dudek, A. Gózdź, N. Schunck, and M. Miśkiewicz, *Phys. Rev. Lett.* **88** (2002), 252502.
- 3) N. Onishi and R. K. Sheline, *Nucl. Phys. A* **165** (1971), 180.
- 4) X. Li and J. Dudek, *Phys. Rev. C* **49** (1994), R1250.
- 5) S. Takami, K. Yabana, and M. Matsuo, *Phys. Lett. B* **431** (1998), 242; M. Matsuo, S. Takami, and K. Yabana, in the proceedings of “Nuclear Structure 98”, Gatlinburg, Tennessee, Aug., 1998, AIP Conference Proceedings 481, p. 345.
- 6) M. Yamagami, K. Matsuyanagi, and M. Matsuo, *Nucl. Phys. A* **693** (2001), 579.
- 7) S. Tagami and Y. R. Shimizu, *Prog. Theor. Phys.* **127** (2012), 79.
- 8) L. M. Robledo, *Phys. Rev. C* **79** (2009), 021302(R).
- 9) T. Sumikama, et al., *Phys. Rev. Lett.* **106** (2011), 202501.
- 10) N. Schunck, J. Dudek, A. Gózdź, and P. H. Regan, *Phys. Rev. C* **69** (2004), 061305(R).
- 11) N. Tajima, Y. R. Shimizu, and S. Takahara, *Phys. Rev. C* **82** (2010), 034316.
- 12) G. Herzberg, *Molecular Spectra and Molecular Structure Vol. II* (D. Van Nostrand Company, New York, 1945).